



1 **Salinity changes and anoxia resulting from enhanced runoff**
2 **during the late Permian global warming and mass extinction**
3 **event**
4

5 Elsbeth E. van Soelen¹, Richard .J Twitchett², Wolfram M. Kürschner³
6

7 ¹University of Oslo, Departments of Geosciences, P.O box 1047 Blindern 0316 Oslo, Norway

8 ²Natural History Museum, Earth Sciences Department, London, SW7 5BD, UK

9 ³Department of Geosciences and Centre for Earth Evolution and Dynamics (CEED), University of Oslo, Oslo,
10 Norway

11

12 *Correspondence to:* Elsbeth E. van Soelen (e.e.v.soelen@geo.uio.no)

13



14 **Abstract.** The Late Permian biotic crisis had a major impact on marine and terrestrial environments. Rising CO₂
15 levels following Siberian Trap volcanic activity were likely responsible for expanding marine anoxia and
16 elevated water temperatures. This study focusses on one of the stratigraphically most expanded Permian-
17 Triassic records known, from Jameson land, east Greenland. High resolution sampling allows for a detailed
18 reconstruction of the changing environmental conditions during the extinction event and the development of
19 anoxic water conditions. Since very little is known about how salinity was affected during the extinction event,
20 we especially focus on the aquatic palynomorphs and infer changes in salinity from changes in the assemblage
21 and morphology. The extinction event, here defined by a peak in spore/pollen, indicating disturbance and
22 vegetation destruction in the terrestrial environment, postdates a negative excursion in the total organic carbon,
23 but predates the development of anoxia in the basin. Based on the newest estimations for sedimentation rates,
24 the marine and terrestrial ecosystem collapse took between 1.6 to 8 kyrs, a much shorter interval than previously
25 estimated. The palynofacies and palynomorph records show that the environmental changes can be explained by
26 enhanced runoff, increased primary productivity and water column stratification. A lowering in salinity is
27 supported by changes in the acritarch morphology. The length of the processes of the acritarchs becomes shorter
28 during the extinction event and we propose that these changes are evidence for a reduction in salinity in the
29 shallow marine setting of the study site. This inference is supported by changes in acritarch distribution, which
30 suggest a change in palaeoenvironment from open marine conditions before the start of the extinction event to
31 more near-shore conditions during and after the crisis. In a period of sea-level rise, such a reduction in salinity
32 can only be explained by increased runoff. High amounts of both terrestrial and marine organic fragments in the
33 first anoxic layers suggest that high runoff, increased nutrient availability, possibly in combination with soil
34 erosion, are responsible for the development of anoxia in the basin. Enhanced runoff could result from changes
35 in the hydrological cycle during the late Permian extinction event, which is a likely consequence of global
36 warming. In addition, vegetation destruction and soil erosion may also have resulted in enhanced runoff.
37 Salinity stratification could potentially explain the development of anoxia in other shallow marine sites. The
38 input of fresh water and related changes in coastal salinity could also have implications for the interpretation of
39 oxygen isotope records and sea water temperature reconstructions in some sites.

40



41 1. Introduction

42 The late Permian extinction event was the most severe global crisis of the Phanerozoic in terms of both
43 taxonomic loss and ecological impact (e.g. McGhee et al., 2012). The current consensus is that the extinction
44 was likely due to global warming and associated environmental changes caused by CO₂ emissions from Siberian
45 Trap volcanic activity, because of the close timing between the volcanic activity and the extinction event (e.g.,
46 Burgess et al., 2017; Burgess and Bowring, 2015). Most studies on the late Permian extinction have inferred that
47 expanding marine anoxia (e.g. Wignall and Hallam, 1992) is a key biotic factor causing marine extinction and
48 ecosystem collapse. There are different theories to explain the spreading of anoxia, which affected both deep
49 and shallow sites (e.g. Bond and Wignall, 2010; Isozaki, 1997; Wignall and Twitchett, 1996). A weakened
50 temperature gradient between equator and pole would have slowed ocean circulation and may have facilitated
51 expansion of the oxygen minimum zone (Hotinski et al., 2001). Increased weathering and detrital input (Algeo
52 and Twitchett, 2010), and soil erosion (Sephton et al., 2005) led to enhanced terrestrial matter input in marine
53 sections, and may also have contributed to eutrophication and in stratified waters led to hypoxia or anoxia
54 (Sephton et al., 2005). Other factors that are thought to play important roles in the extinction are elevated water
55 temperatures (e.g. Sun et al., 2012), and ocean acidification (Clapham and Payne, 2011). One important
56 environmental parameter that has received relatively little attention is salinity, even though low salinity ocean
57 conditions were once considered to be a leading cause of the marine extinction (Fischer, 1964; Stevens, 1977).
58 Furthermore, potential impacts of changes in salinity, which might be expected from enhanced discharge of
59 freshwater into shelf seas (Winguth and Winguth, 2012), have been largely ignored.

60 Microfossils of marine algae are excellent recorders of environmental change in the water column. Of
61 these, the organic-walled cysts of dinoflagellates have proven especially useful in palaeo-environmental studies
62 (e.g. Ellegaard, 2000; Mertens et al., 2009, 2012, Mudie et al., 2001, 2002; Sluijs and Brinkhuis, 2009; Vernal et
63 al., 2000). While dinocysts are absent or sparse in Palaeozoic deposits, acritarchs are commonly recorded (e.g.
64 Tappan and Loeblich, 1973), even during the late Permian when acritarch diversity was declining (Lei et al.,
65 2013b). Acritarchs are a group of microfossils of organic composition and unknown affinity (Evvitt, 1963). Many
66 acritarchs are, however, found exclusively in marine rocks, and some are thought to be precursors of modern
67 dinoflagellate cysts (e.g. Servais et al., 2004). Several studies in East Greenland have reported fluctuating
68 abundances of acritarchs during the Late Permian and Early Triassic (e.g. Balme, 1979; Piasecki, 1984;
69 Stemmerik et al., 2001), but very few late Permian studies have documented the relative abundance of the
70 different genera of aquatic palynomorphs (for example, Shen et al., 2013). Similar to dinocysts, acritarch
71 morphology has been linked to environmental conditions, and acritarchs with longer processes are generally
72 more abundant in more open marine settings (Lei et al., 2012; Stricanne et al., 2004). Both dinocyst and
73 acritarch studies show that salinity is an important, albeit not the only, factor that influences cyst morphology. It
74 is thought that the longer processes in higher salinities stimulate clustering with other cysts or particles in the
75 water column, and thus enhance sinking to the seafloor (Mertens et al., 2009).

76 The rock record of Jameson Land, East Greenland, has provided key insights into marine environmental
77 changes during the late Permian extinction event. Previous work on this section by Twitchett et al. (2001)
78 showed that collapse of marine and terrestrial ecosystems was synchronous and took between 10 to 60 kyr.
79 Palynological work by Looy et al. (2001) showed that the terrestrial ecosystem collapse is characterized by a



80 distinct rise in spores, indicative of the loss of woodland and increase in disturbance taxa. The onset of anoxic
81 conditions is not as abrupt at this location as seen in some other sections, but instead Wignall and Twitchett,
82 (2002) found unusual alternating patterns of bioturbated and laminated siltstones in the top of the Schuchert Dal
83 Formation and lowest of the Wordie Creek Formation (Fig. 1). In a recent study, Mettam et al., (2017) showed
84 that rapidly fluctuating redox conditions occurred during the late Permian extinction, while sedimentological
85 observations imply that sea level was rising in this period. Estimations of sedimentation rates indicate that each
86 bioturbated/laminated rock interval, which are between 2-10 cm thick, have been deposited in a period of 50-
87 1000 years (Mettam et al., 2017). To study the environmental conditions associated with the deposition of these
88 sediments we look in detail at a short (9 m) interval covering the late Permian extinction and the Formation
89 boundary between the Schuchert Dal and Wordie Creek Formation. Palaeoenvironment is studied by looking at
90 variations in the palynofacies (organic particles) and the acritarch assemblage. In addition we present a record of
91 morphological changes within the acritarch *Michrhystridium*. Runoff and erosion, salinity, sea-level fluctuations
92 and temperature rise are discussed as possible reasons for the changing environmental conditions.

93

94 2. Geological setting and stratigraphy

95 Samples were collected at the Fiskegrav location of Stemmerik et al. (2001), an outcrop in East Greenland
96 (N71°32'01.6", W024°20'03.0"), in a small stream section on the east side of Schuchert Dal (Fig. 1). The
97 section was deposited within a relatively narrow, north-south oriented basin (Stemmerik et al., 2001; Wignall
98 and Twitchett, 2002). Active rifting and rapid subsidence has resulted in the deposition of one of the most
99 expanded P-Tr sections. At the Fiskegrav location there are no obvious breaks in sedimentation, even though
100 large erosive channels exist in P-Tr sections in more northern locations (Twitchett et al., 2001; Wignall and
101 Twitchett, 2002).

102 The Fiskegrav section shows a transition from the Schuchert Dal Formation into the Wordie Creek
103 Formation. The Permian/Triassic boundary, defined by the first occurrence of the conodont *Hindeodus parvus*
104 (Yin, 1996), is located at 23.5 m above the base of the Wordie Creek Formation (Twitchett et al., 2001). This
105 study focusses on a ca. 9 m section interval including the late Permian extinction and the formation boundary
106 (Fig. 1). The upper part of the Schuchert Dal Formation consists of blocky (bioturbated), micaceous, greenish
107 mudstones (muddy siltstones), whereas the lower Wordie Creek Formation consists mainly of laminated, dark
108 grey mudstones (clay-siltstones) that often contain framboidal pyrite (Twitchett et al., 2001; Wignall and
109 Twitchett, 2002). The extinction event occurs in the upper metres of the Schuchert Dal Formation, and the start
110 of the biotic crisis is synchronous in marine and terrestrial ecosystems (Looy et al., 2001; Twitchett et al., 2001).
111 For more details on biostratigraphy see Mettam et al., (2017); Stemmerik et al., (2001) and Twitchett et al.,
112 (2001).

113

114 3. Material and Method

115 3.1 Material



116 A total of 36 samples were collected from the top 4.5m of the Schuchert Dal Formation and the lower 4.2m of
117 the Wordie Creek Formation. Sample resolution is highest (10cm intervals) in the 2.5m interval covering the
118 formation boundary and the extinction event. Depths are given in m, relative to the formation boundary between
119 Schuchert Dal and Wordie Creek Fm. Some of the samples used in this study were also analysed by Mettam et
120 al. (2017) during their study of changes in redox conditions at the formation boundary.

121

122 3.2 palynofacies and palynological analysis

123 Samples (of ca.5 g) were crushed, and a tablet with a known amount of lycopodium spores was added
124 to allow quantification of organic particles and palynomorphs. Samples were then treated with hydrochloric acid
125 and hydrofluoric acid to remove carbonates and silicates, and subsequently sieved through 7 µm sieves. Heavy
126 liquid separation was used to remove heavy minerals like pyrite. The residue, containing palynomorphs and
127 other organic particles, was mounted onto microscope slides. Material was counted using a Leitz Diaplan
128 microscope and an AxioCam ERc 5s camera attached to a computer with Zen microscope software (Zen 2 lite,
129 2011). A minimum of 300 particles per sample were counted for palynofacies analyses. Aquatic palynomorphs
130 were counted to reach 100 specimens when abundant and at least 30 specimens when abundance was low. Still,
131 due to low abundances during the biotic crisis, in some samples counts were below 30 (these 6 samples are
132 indicated in Fig. 4).

133

134 3.3 Acritarch measurements

135 The genus *Michrhystridium* includes many species, of which ca. 20 are known from the Permian-
136 Triassic interval, which differ in their body size, number of processes and process length (Lei et al., 2013b;
137 Sarjeant, 1970). Only those with a spherical central body and many (>10) simple processes with closed tips
138 were included in this study (i.e. the *M. breve* Group, according to Lei et al., 2013b). Thus, amongst others, *M.*
139 *pentagonale* was excluded. Specimens were excluded if they were too damaged (folded or broken) to allow
140 measurements. To counteract the effects of compression (which can make the body look longer), body size was
141 calculated from the average of two linear measurements perpendicular to each other. For each specimen three
142 processes were measured (all within one focal plane). The aim was to measure 20-30 specimens per sample, but
143 acritarch concentrations were low during the biotic crisis interval, and therefore 5 samples had lower counts
144 (indicated in Fig. 6).

145

146 4. Results

147 4.1 Palynofacies

148 The most abundant organic particles are phytoclasts and amorphous organic matter (AOM) which together
149 comprise 45 to 90% of the palynofacies (Fig. 2). Phytoclasts are dominant in the bioturbated samples in the



150 lower part of the section, while AOM dominates the palynofacies in the laminated intervals. Other terrestrially
151 derived organic (wood fragments and charcoal) particles make up a small portion (<20%) of the palynofacies
152 and are not influenced by the alternating anoxic/oxic depositional conditions (Fig. 2). Palynomorphs were
153 divided into three groups: pollen, spores and aquatic palynomorphs. Pollen abundance relative to other
154 palynofacies is higher in the upper 0.5 m of the Schuchert Dal Formation and lowest metre of the Wordie Creek
155 Formation (5-20%), which is mainly caused by the high number of pollen fragments (sacci) during and
156 following the extinction event (Fig. 2). Spores have highest abundance in the upper metre of the Schuchert Dal
157 Formation (up to 35%), where also the spore/pollen ratio is highest. Aquatic palynomorphs (acritarchs and other
158 algal remains like *Tasmanites* and *Cymatiosphaera*) make up a very small fraction of the palynofacies in the
159 Schuchert Dal Formation (<2%), but become relatively more abundant in the Wordie Creek Formation (up to
160 14%).

161

162 4.2 Aquatic palynomorphs

163 Although Permian acritarch diversity is considered to be low, an overview of Permian phytoplankton by Lei et
164 al. (2013b) showed a richness of about 20-30 genera during most of the Permian, with acritarchs belonging to
165 the genera *Micrhystridium* and *Veryhachium* being the most common (Lei et al., 2013b, 2013a; Sarjeant and
166 Stancliffe, 1994). Since cysts are generally small in size it is difficult to study them under light microscope and
167 identification at species level can be difficult (Sarjeant, 1970). Several revisions and simplifications have been
168 proposed for the genera (Lei et al., 2013a; Sarjeant and Stancliffe, 1994). We follow the simple classification
169 scheme proposed by Lei et al. (2013a), in which different species of acritarchs are grouped together, based on
170 geometrical shape of the acritarchs. Photos of selected aquatic palynomorphs are shown in the plate of Fig. 3.

171 Concentrations of aquatic palynomorphs were on average ca.4 times higher in the laminated rocks
172 compared to the bioturbated rocks (Fig. 4). Acritarch abundance also declines during the extinction event. The
173 majority (25 - 100%) of the acritarchs belong to the *Micrhystridium breve* Group (Fig. 4). This group includes
174 all acritarchs with a spherical central body and numerous processes. The *Veryhachium laidii* Group (acritarchs
175 with a rectangular central body shape), the *V. trispinosum* Group (triangular shape), *V. cylindricum* Group
176 (ellipsoidal shape) and *M. pentagonale* Group (pentagonal or hexagonal shape) were mostly found in
177 bioturbated intervals of the upper part of the Schuchert Dal Formation, especially just before and during the
178 extinction interval (Fig. 4). The leiospheres include all aquatic palynomorphs with a spherical shape and either a
179 smooth surface or with small ornamentation, but no processes. The highest abundances (up to 70%) of
180 leiospheres are found in the laminated sediments of the Wordie Creek Formation (Fig. 4). *Cymatiosphaera* are
181 rare in the record and found in both the oxidized siltstones of the Schuchert Dal Formation, but also in some
182 intervals in the laminated siltstones. *Tasmanites* were found only in one sample, also during the marine
183 extinction phase. The apparent relatively higher abundance of *Cymatiosphaera* and *Tasmanites* in the top of the
184 Schuchert Dal Formation is a consequence low total count of the aquatic palynomorphs during the extinction
185 event. The most diverse samples were found in the bioturbated rocks of the upper metre of the Schuchert Dal
186 Formation, an interval that partly overlaps with the extinction interval.



187 The *Micrhystridium* Group has a diverse morphology, and shows variation in vesicle size and number
188 of processes. Most of the measured specimens are very similar to the species *M. breve* as described by Jansonius
189 (1962) in both the number and shape of the processes. However, the size of the central body and the length of
190 the processes of many of the measured acritarchs fall outside of the defined size-range of *M. breve*. The
191 distributions of both body size and process length are unimodal (Fig. 5), which strongly suggests that the
192 measured specimens all belong to a single species of *Micrhystridium*. Body size is variable and in the two-metre
193 interval spanning the formation boundary, acritarchs in the laminated rocks are on average larger compared to
194 those in the bioturbated rocks (Fig. 6). Process length decreases gradually from the start of the extinction event
195 until its end, and then remains shorter through to the top of the studied section. Process length not only changes
196 in absolute terms, but also relatively to the size of the body.

197

198 **5. Discussion**

199 **5.1 The extinction event and onset of anoxia**

200 Consistent with the results of Looy et al. (2001), we find a strong increase in spores, relative to pollen,
201 in the upper Schuchert Dal Formation (Fig. 2). Since this peak in spores coincides with the interval of marine
202 ecosystem collapse defined by Twitchett et al. (2001), we define the period with highest spore/pollen ratios as
203 the extinction interval. Twitchett et al. (2001) found large changes in marine plankton abundance in their study
204 of the Fiskegrav section, with a bloom just before the disappearance of trace fossils, followed by almost
205 complete absence of acritarchs immediately after the collapse of the marine ecosystem. This phytoplankton
206 bloom is not obvious in our higher resolution data, and may simply be an artefact of the relatively low-
207 resolution sampling of Twitchett et al., (2001), but the number of acritarchs is indeed greatly reduced during the
208 biotic crisis (Fig. 4). The peak in spore/pollen and decrease in acritarch abundance occurs in an interval of ca.
209 0.8m, which is comparable to the interval found by Twitchett et al., (2001) for marine and terrestrial ecosystem
210 collapse. Twitchett et al., (2001) estimated the collapse to have taken between 10 and 60 kyrs, however, recently
211 improved estimations of sedimentation rates in the Fiskegrav section (Mettam et al 2017) now give an estimated
212 duration of between 1.6 to 8 kyrs for the marine and terrestrial ecosystem collapse.

213 During the start of the biotic crisis rocks remain bioturbated but within the upper 0.5 m of the
214 Schuchert Dal Formation there are intervals with laminated rocks (Fig. 2), indicative for anoxia (Twitchett et al.,
215 2001). AOM, which is structureless organic matter, is dominant in the laminated rocks. AOM can derive from
216 degraded macrophyte, phytoplankton or higher plant tissue, or it may also be bacterially derived (Tyson, 1995).
217 Anoxic conditions can stimulate the production of marine AOM (Pacton et al., 2011), but also result in better
218 preservation after sedimentation (Tyson, 1995). The relative proportions of AOM versus phytoclasts thus
219 indicate the amount of oxygenation of the depositional environment (Tyson, 1995). A recent, high-resolution
220 study of the $\delta^{13}\text{C}$ of total organic carbon (TOC) by Mettam et al., (2017) shows a negative shift of 5-6‰ that
221 begins 1.80m below the top of the Schuchert Dal Formation at Fiskegrav, (Fig. 2). The onset of this negative
222 excursion coincides closely with the last occurrence of Permian macroinvertebrate fossils (Mettam et al., 2017),
223 but pre-dates the collapse of marine and terrestrial ecosystems defined by disappearance of bioturbation.



224 Mettam et al. (2017) record a small, but consistent, offset in $\delta^{13}\text{C}$ values between the laminated/bioturbated
225 intervals (Fig. 2). This offset can be explained by the differences in organic matter source, which is mostly
226 phytoclasts (terrestrial) in the bioturbated intervals while AOM (marine and terrestrial) dominates in the
227 laminated intervals. However, the main shift is not associated with major changes in the palynofacies, and
228 occurs in a part of the section where the palynofacies mainly consist of terrestrially derived organic matter (Fig.
229 2). This negative shift in carbon isotopes associated with the late Permian extinction event is recognized
230 worldwide (e.g. Korte and Kozur, 2010) and usually precedes, the extinction event (e.g. Burgess and Bowring,
231 2015; Korte and Kozur, 2010). It has been interpreted as resulting from atmospheric changes in $\delta^{13}\text{C}$ values,
232 which can be directly, or indirectly, related to Siberian trap volcanism (e.g. Cui and Kump, 2015; Svensen et al.,
233 2009).

234 Mettam et al. (2017) studied redox conditions in the same section and showed that conditions became
235 potentially anoxic, and ferruginous (Fe^{2+} - rich) in the laminated intervals near the formation boundary. Within
236 the lowermost Wordie Creek Formation, from 0.6-0.7 m above the formation boundary, anoxic conditions are
237 confirmed by Fe speciation (Mettam et al., 2017). Since the extinction started before conditions became
238 ferruginous, spreading anoxia cannot be the main cause for the marine biotic crisis in the Fiskegrav section.
239 Grasby et al. (2015) distinguished three phases of extinction in the shallow marine sequence of Festningen
240 (Svalbard): first is the loss of carbonate macrofauna, followed by loss of siliceous sponges, and finally a loss of
241 all trace fossils. Thus, similar to what is observed in East Greenland, the first laminated sediments do not
242 represent the start of the biotic crisis. This is unsurprising as expanding marine hypoxia is a predicted
243 consequence of global warming, which was probably caused by elevated CO_2 flux from Siberian Trap
244 volcanism (Benton and Twitchett, 2003; Grard et al., 2005). Therefore, extinctions that occurred prior to the
245 appearance of widespread anoxia were more likely due to the direct, short-term effects of volcanic activity (e.g.
246 metal toxicity), or the more immediate effects of CO_2 rise or temperature increase. The laminated rocks are
247 associated with higher amount of pollen fragments (Fig. 2), which could be an indication for elevated terrestrial
248 organic matter input (e.g. soil erosion), while the higher amount of AOM can be partly explained by terrestrial
249 organic matter input, and partly by increased marine productivity and better preservation of organic matter due
250 to low oxygen conditions. Increased weathering and run-off are expected consequences of atmospheric and
251 hydrological changes associated with global warming. Algeo and Twitchett, (2010) demonstrated that sediment
252 accumulation rates greatly increased in shallow shelf seas in the latest Permian and earliest Triassic, consistent
253 with enhanced weathering and run-off, and Sephton et al. (2005) found evidence for large-scale soil erosion.

254

255 5.2 Sea-level and salinity changes

256 If the laminated rocks are indeed a consequence of enhanced runoff, this is expected to affect also
257 marine environmental conditions, such as a decrease in (surface) salinity. At the same time, sea-level
258 fluctuations at and near the boundary need to be considered, since these would also affect marine environmental
259 conditions and could potentially affect salinity. The Fiskegrav section has well preserved aquatic palynomorphs,
260 and their diversity, distribution and morphology can provide valuable information on marine environmental
261 changes. Palaeozoic studies have shown that acritarch diversity is generally higher in deeper, more distal



262 settings (e.g. Lei et al., 2012; Stricanne et al., 2004). In addition, different studies have shown that *Veryhachium*
263 favoured more open marine settings, while *Micrhystridium* favoured near-shore environments (e.g. Wall 1965,
264 Lei et al., 2012). It is possible that some of the leiospheres in the Fiskegrav section belong to the genus
265 *Leiosphaeridia*, as the dimensions are comparable to *L. microgranifera* and *L. minutissima* that were found in
266 Chinese Permian-Triassic sections (Lei et al., 2012), but the small ornamentations on both of those species is
267 different (Fig. 3). In these Chinese Permian sections the *Leiosphaeridia* are associated with deeper/more open
268 marine waters (Lei et al., 2012). On the other hand, studies of early Palaeozoic acritarchs show that, in general,
269 leiospheres, or sphaeromorphs, are most frequent in proximal environments (Li et al., 2004; Stricanne et al.,
270 2004). The leiosphere-group might be polyphyletic and some species might have prasinophyte affinities
271 (Colbath and Grenfell, 1995), which complicates their use for environmental reconstructions. Whatever the
272 biological origin of the leiosphere is, in this study site they apparently favoured the palaeoenvironmental
273 conditions associated with the deposition of the laminated rocks, starting during the extinction event.

274 In the Fiskegrav section, the decline in diversity from the upper Schuchert Dal Formation to the Wordie
275 Creek formation, together with the change in assemblage from *Veryhachium/Micrhystridium* to
276 *Micrhystridium*/leiosphere dominance could thus be interpreted as a change from a distal to a more proximal
277 setting, which would suggest a marine regression. Although this was once considered as a possible cause of the
278 late Permian extinction event (Hallam and Cohen, 1989), the current consensus is that eustatic sea-level fall
279 occurred prior to collapse of marine ecosystems and the extinction, and the subsequent transition from the
280 Permian to the Triassic happened during sea-level rise (Wignall and Hallam, 1992). In some East Greenland
281 locations, apparently missing biozones and local erosive conglomeratic channels have been proposed as
282 evidence for sea-level fall near the boundary between the Schuchert Dal and Wordie Creek formations (Surlyk
283 et al., 1984), but Wignall and Twitchett (2002) demonstrated that in central Jameson Land the sedimentological
284 changes are consistent with sea-level rise, and that the erosive, conglomeratic channels occur at multiple
285 stratigraphic levels and postdate the extinction and Permian/Triassic boundary.

286 Thus, during the extinction event the acritarch assemblage changes to a more typical near-shore
287 assemblage, despite the ongoing sea-level rise. Instead of a marine regression, the observed shift in acritarch
288 assemblages could be explained by an increase in runoff which affects the near-shore environment by lowering
289 surface water salinity and delivering nutrients, both of which are found to affect the distribution of modern
290 phytoplankton (e.g. Bouimetarhan et al., 2009; Devillers and de Vernal, 2000; Pospelova et al., 2004; Zonneveld
291 et al., 2013). Dinocyst morphology has also been linked to environmental conditions (e.g., Mertens et al., 2009,
292 2011), with salinity identified as an important factor influencing process length (Ellegaard et al., 2002; Mertens
293 et al., 2011). Similarly, studies of acritarch process length and palaeoenvironment show that species and
294 individuals with longer processes are generally found in more offshore locations, while in inshore settings
295 acritarchs with shorter processes are more abundant (Lei et al., 2013a; Servais et al., 2004; Stricanne et al.,
296 2004). The average process length of specimens belonging to the *Micrhystridium breve* Group, show a
297 decreasing trend during the extinction interval, with higher values before the extinction event, and lower values
298 after the event (Fig. 6), which could thus be interpreted as a lowering in salinity during the extinction event.
299 Within the 2m interval including the extinction interval (-1 – +1m) there is also a consistent offset in body size
300 between samples from bioturbated and laminated rocks. The body size of some dinocysts has been found to vary
301 with temperature and salinity (e.g. Ellegaard et al., 2002; Mertens et al., 2012), however, the relation has not



302 been well studied. Possibly low oxygen or salinity conditions or increased nutrient availability influenced
303 acritarch body size in this interval. Runoff, lower salinity, and salinity stratification together can explain the
304 observed changes in palynofacies and acritarch records. The changed environmental conditions continued
305 through the aftermath of the biotic crisis, as shown by persistently low process lengths to the end of the study
306 interval (Fig. 6). Meanwhile, the ongoing marine transgression likely resulted in the shoreward migration of
307 oxygen deficient waters which explain the development of permanently anoxic conditions higher up in the
308 Wordie Creek Formation (over 0.6-0.7 m from the Fm boundary) (Mettam et al., 2017).

309 The development of widespread anoxia in the late Permian is usually explained by an expansion of
310 anoxic deep waters onto the shelf (e.g. Grasby and Beauchamp, 2009). However, increased runoff and the
311 development of estuarine circulation provide an alternative explanation for the development of anoxia in some
312 shallow marine environments. Furthermore, low salinity is known to negatively impact biomass and size of
313 modern marine invertebrates (e.g. Westerborg et al., 2002), and, along with higher temperatures and hypoxia,
314 might also be a contributing factor in the size reduction of marine organisms recorded in the aftermath of the
315 late Permian extinction event, such as observed for the bivalve *Claraia* the Permian-Triassic section of East-
316 Greenland (Twitchett, 2007). Low salinity conditions have previously been invoked to explain the dominance of
317 the brachiopod lingulid in post-extinction ecosystems (Zonneveld et al., 2007), because they are able to tolerate
318 a wide range of salinities as well as hypoxia (e.g. Hammen and Lum, 1977). Lingulid fossils are found in many
319 Permian-Triassic (shallow) marine sections (e.g. Peng et al., 2007) and the lowering of salinities in shallow
320 marine settings and spreading anoxia provided ecological space for the lingulids (Peng et al., 2007; Rodland and
321 Bottjer, 2001). It has been suggested that rising sea water temperatures in the Tethys, resulted in strengthened
322 monsoonal activity (e.g. Winguth and Winguth, 2012) and enhanced precipitation and runoff in the areas
323 surrounding the Tethys (e.g. Parrish et al., 1982). Whether this would have had an effect on the study site is
324 questionable, because of its distance to the Tethys and relatively sheltered, inland position. Possibly river
325 systems existed which brought freshwater to the Greenland-Norway basin from the South. It is also possible that
326 rainfall increased locally. Mettam et al., (2017) speculated that changes in circulation patterns may have resulted
327 in onshore winds bringing moist air to the study site. In addition vegetation destruction and soil erosion may
328 also have contributed to enhanced runoff.

329

330 **5.3 Sea water temperature**

331 Besides salinity, increasing water temperatures can also affect process length in dinocysts (e.g. Mertens
332 et al., 2009, 2012) but this relationship is not always evident (e.g. Ellegaard et al., 2002). Sea water temperature
333 reconstructions for the late Permian and Early Triassic exist mainly from carbonate rich sections originating in
334 the Tethys Ocean (e.g. Joachimski et al., 2012; Schobben et al., 2014; Sun et al., 2012). These reconstructions
335 indicate increasing temperatures during the extinction event, and maximum temperatures are reached in the
336 Early Triassic (e.g. Joachimski et al., 2012; Kearsley et al., 2009; Schobben et al., 2014; Sun et al., 2012). Since
337 no water temperature reconstructions exist for the Greenland-Norway basin, at this time, it is not possible to
338 exclude the effects of rising water temperatures on the acritarch morphology. Increasing water temperatures
339 might be partly responsible for decreasing process length in acritarchs, however, a rising sea-level in



340 combination with rising temperatures are not able to explain the changes in the acritarch assemblages, which
341 indicate a shift from more open marine to near-shore conditions. Increased runoff cannot only explain the
342 reconstructed changes in palynofacies and acritarch records, but in addition, a reduction in salinity also has
343 significant implications for palaeotemperature reconstructions calculated from the oxygen isotopes of carbonates.
344 Most Permian-Triassic temperature records are from the Tethys or surrounding areas, where monsoon activity
345 has been proposed to increase (Winguth and Winguth, 2012) and thus salinity is expected to change as well.
346 Permian-Triassic oxygen isotope data for palaeotemperature estimates have been derived from brachiopod shells
347 (Kearsey et al., 2009) or conodont apatite (Joachimski et al., 2012; Schobben et al., 2014), with all studies
348 concluding that temperature rose through the extinction event and that Early Triassic seas were 'lethally hot'
349 (Sun et al., 2012). Oxygen isotope values partially reflect seawater salinity, although this is generally ignored in
350 palaeotemperature studies, because there is currently no independent proxy of salinity change, and so it is
351 assumed that salinity remained constant. If salinity was reduced in shelf seas due to hydrological changes (e.g.
352 enhanced precipitation and run-off), as it appears for East Greenland at least, then all of these studies may have
353 significantly over-estimated Early Triassic temperatures. The actual temperature rise associated with the
354 extinction event would have been lower and below 'lethal' levels, which is more consistent with fossil evidence
355 that the oceans were not completely devoid of life.

356

357 **6. Conclusions**

358 The highest resolution palynological sampling yet attempted for the Fiskegrav location of central Jameson Land
359 has shown significant, millennial-scale changes in marine and terrestrial environments. The biotic crisis,
360 defined by a peak in the spore/pollen ratio which indicates widespread disruption and collapse of the terrestrial
361 flora, postdates the onset of the carbon-isotope excursion. The spore/pollen peak spans 0.8 m of section, which,
362 on current age estimates, gives an estimation of 1600 to 8000 years for the ecosystem collapse. This is much
363 shorter than previous estimations. The onset of the biotic crisis does not appear to coincide with any obvious
364 changes in lithology or sedimentary facies, and deposition of the shallow marine shelf sediments appears to have
365 taken place under oxygenated waters. During the latter stages of the biotic crisis, laminated beds begin to appear,
366 indicating periodic anoxic deposition. These laminated rocks contain palynological evidence for a more near-
367 shore setting, which contradicts the widely accepted evidence that globally sea-level was actually rising during
368 the extinction event. A preferred alternative explanation, consistent with palynological assemblages, is that
369 enhanced runoff, water column stratification and enhanced primary productivity led to the development of
370 anoxic bottom waters. Enhanced runoff would lead to elevated freshwater flux into shallow shelf seas, which
371 would have led to the development of a freshwater wedge, stratification and a reduction in salinity. Acritarch
372 process length is considered here to be a proxy for seawater salinity, and supports these inferred changes.
373 Increased runoff did not immediately lead to anoxia, possibly because precipitation gradually increased during
374 the extinction event until the freshwater flow was large enough to cause water column stratification. Increasing
375 sea water temperatures may have also affected acritarch morphology, and partially be responsible for the
376 reduced process length. However, rising temperatures alone cannot explain the reconstructed changes in the
377 palynofacies and acritarch records. In fact, sea water temperature reconstructions may overestimate the rise in



378 water temperatures during the extinction event, since possible changes in salinity are not included in the
379 calculations.

380

381 **7. Data availability.** The data reported in this paper is available in tables in the supplementary files.

382

383 **Author contributions.** WMK designed the study. RJT provided material. EEvS analysed the samples for
384 palynofacies and palynomorph content and performed measurements on acritarchs. EEvS wrote the paper with
385 input from WMK and RJT.

386

387 **Competing interests.** The authors declare that they have no conflict of interest.

388

389 **Acknowledgements**

390 This work was funded by the Norwegian Research Council, project 234005, The Permian/Triassic evolution of
391 the Timan-Pechora and Barents Sea Basins. We thank B.L. Berg and M.S. Naoroz for technical support.
392 Samples were collected by RJT, who thanks G. Cuny and the Danish National Research Foundation for logistic
393 and financial support.

394

395 **References**

396 Algeo, T. J. and Twitchett, R. J.: Anomalous Early Triassic sediment fluxes due to elevated weathering rates and
397 their biological consequences, *Geology*, 38(11), 1023–1026, doi:10.1130/G31203.1, 2010.

398 Algeo, T. J., Heckel, P. H., Maynard, J. B., Blakey, R. and Rowe, H.: Modern and ancient epeiric seas and the
399 super-estuarine circulation model of marine anoxia, *Dynamics of Epeiric seas: sedimentological, paleontological*
400 *and geochemical perspectives*. Geological Association Canada Special Publication, 7–38, 2008.

401 Balme, B. E.: Palynology of Permian-Triassic boundary beds at Kap Stosch, East Greenland, *Nyt nordisk forlag*,
402 200(6), 1979.

403 Benton, M. J. and Twitchett, R. J.: How to kill (almost) all life: the end-Permian extinction event, *Trends in*
404 *Ecology & Evolution*, 18(7), 358–365, doi:10.1016/S0169-5347(03)00093-4, 2003.

405 Bond, D. P. G. and Wignall, P. B.: Pyrite framboid study of marine Permian–Triassic boundary sections: A
406 complex anoxic event and its relationship to contemporaneous mass extinction, *GSA Bulletin*, 122(7–8), 1265–
407 1279, doi:10.1130/B30042.1, 2010.

408 Bouimetarhan, I., Marret, F., Dupont, L. and Zonneveld, K.: Dinoflagellate cyst distribution in marine surface
409 sediments off West Africa (17–6°N) in relation to sea-surface conditions, freshwater input and seasonal coastal
410 upwelling, *Mar. Micropaleontol.*, 71(3–4), 113–130, doi:10.1016/j.marmicro.2009.02.001, 2009.

411 Burgess, S. D. and Bowring, S. A.: High-precision geochronology confirms voluminous magmatism before,
412 during, and after Earth's most severe extinction, *Science Advances*, 1(7), e1500470,
413 doi:10.1126/sciadv.1500470, 2015.



- 414 Burgess, S. D., Muirhead, J. D. and Bowring, S. A.: Initial pulse of Siberian Traps sills as the trigger of the end-
415 Permian mass extinction, *Nat. Commun.*, 8(1), 164, doi:10.1038/s41467-017-00083-9, 2017.
- 416 Clapham, M. E. and Payne, J. L.: Acidification, anoxia, and extinction: A multiple logistic regression analysis of
417 extinction selectivity during the Middle and Late Permian, *Geology*, 39(11), 1059–1062, doi:10.1130/G32230.1,
418 2011.
- 419 Colbath, G. K. and Grenfell, H. R.: Review of biological affinities of Paleozoic acid-resistant, organic-walled
420 eukaryotic algal microfossils (including “acritarchs”), *Rev. Palaeobot. Palyno.*, 86(3–4), 287–314,
421 doi:10.1016/0034-6667(94)00148-D, 1995.
- 422 Cui, Y. and Kump, L. R.: Global warming and the end-Permian extinction event: Proxy and modeling
423 perspectives, *Earth-Science Reviews*, 149, 5–22, doi:10.1016/j.earscirev.2014.04.007, 2015.
- 424 Devillers, R. and de Vernal, A.: Distribution of dinoflagellate cysts in surface sediments of the northern North
425 Atlantic in relation to nutrient content and productivity in surface waters, *Mar. Geol.*, 166(1), 103–124,
426 doi:10.1016/S0025-3227(00)00007-4, 2000.
- 427 Ellegaard, M.: Variations in dinoflagellate cyst morphology under conditions of changing salinity during the last
428 2000 years in the Limfjord, Denmark, *Rev. Palaeobot. Palyno.*, 109(1), 65–81, doi:10.1016/S0034-
429 6667(99)00045-7, 2000.
- 430 Ellegaard, M., Lewis, J. and Harding, I.: Cyst–theca relationship, life cycle, and effects of temperature and
431 salinity on the cyst morphology of *Gonyaulax Baltica* Sp. Nov. (dinophyceae) from the Baltic Sea Area, *J.*
432 *Phycol.*, 38(4), 775–789, doi:10.1046/j.1529-8817.2002.01062.x, 2002.
- 433 Evitt, W. R.: A discussion and proposals concerning fossil dinoflagellates, hystrichospheres, and acritarchs, I,
434 *PNAS*, 49(2), 158–164, 1963.
- 435 Fischer, A. G.: Brackish oceans as the cause of the Permo-Triassic marine faunal crisis, in *Problems in*
436 *Palaeoclimatology*, edited by A. E. M. Nairn, pp. 566–574, Interscience, London., 1964.
- 437 Grard, A., François, L. M., Dessert, C., Dupré, B. and Goddérés, Y.: Basaltic volcanism and mass extinction at
438 the Permo-Triassic boundary: Environmental impact and modeling of the global carbon cycle, *Earth and*
439 *Planetary Science Letters*, 234(1), 207–221, doi:10.1016/j.epsl.2005.02.027, 2005.
- 440 Grasby, S. E. and Beauchamp, B.: Latest Permian to Early Triassic basin-to-shelf anoxia in the Sverdrup Basin,
441 Arctic Canada, *Chem. Geol.*, 264(1–4), 232–246, doi:10.1016/j.chemgeo.2009.03.009, 2009.
- 442 Grasby, S. E., Beauchamp, B., Bond, D. P. G., Wignall, P., Talavera, C., Galloway, J. M., Piepjohn, K.,
443 Reinhardt, L. and Blomeier, D.: Progressive environmental deterioration in northwestern Pangea leading to the
444 latest Permian extinction, *Geol. Soc. Am. Bull.*, B31197.1, doi:10.1130/B31197.1, 2015.
- 445 Hallam, A. and Cohen, J. M.: The Case for Sea-Level Change as a Dominant Causal Factor in Mass Extinction
446 of Marine Invertebrates [and Discussion], *Philos. T. Roy. Soc. B*, 325(1228), 437–455, doi:10.2307/2396934,
447 1989.
- 448 Hammen, C. S. and Lum, S. C.: Salinity tolerance and pedicle regeneration of *Lingula*, *J. Paleontol.*, 51(3), 548–
449 551, 1977.
- 450 Hotinski, R. M., Bice, K. L., Kump, L. R., Najjar, R. G. and Arthur, M. A.: Ocean stagnation and end-Permian
451 anoxia, *Geology*, 29(1), 7–10, doi:10.1130/0091-7613(2001)029<0007:OSAEP>2.0.CO;2, 2001.
- 452 Isozaki, Y.: Permo-Triassic Boundary Superanoxia and Stratified Superocean: Records from Lost Deep Sea,
453 *Science*, 276(5310), 235–238, doi:10.1126/science.276.5310.235, 1997.
- 454 Jansonius, J.: Palynology of permian and triassic sediments, Peace River area, Western Canada, *Palaeontogr.*
455 *Abt. B*, 35–98, 1962.



- 456 Joachimski, M. M., Lai, X., Shen, S., Jiang, H., Luo, G., Chen, B., Chen, J. and Sun, Y.: Climate warming in the
457 latest Permian and the Permian–Triassic mass extinction, *Geology*, 40(3), 195–198, doi:10.1130/G32707.1,
458 2012.
- 459 Kearsey, T., Twitchett, R. J., Price, G. D. and Grimes, S. T.: Isotope excursions and palaeotemperature estimates
460 from the Permian/Triassic boundary in the Southern Alps (Italy), *Palaeogeogr. Palaeoclimatol., 279(1–2)*, 29–40,
461 doi:10.1016/j.palaeo.2009.04.015, 2009.
- 462 Korte, C. and Kozur, H. W.: Carbon-isotope stratigraphy across the Permian–Triassic boundary: A review, *J.*
463 *Asian Earth Sci.*, 39(4), 215–235, doi:10.1016/j.jseas.2010.01.005, 2010.
- 464 Lei, Y., Servais, T., Feng, Q. and He, W.: The spatial (nearshore–offshore) distribution of latest Permian
465 phytoplankton from the Yangtze Block, South China, *Palaeogeogr. Palaeoclimatol.*, 363–364, 151–162,
466 doi:10.1016/j.palaeo.2012.09.010, 2012.
- 467 Lei, Y., Servais, T., Feng, Q. and He, W.: Latest Permian acritarchs from South China and the
468 *Micrhystridium/Veryhachium* complex revisited, *Palynology*, 37(2), 325–344,
469 doi:10.1080/01916122.2013.793625, 2013a.
- 470 Lei, Y., Servais, T. and Feng, Q.: The diversity of the Permian phytoplankton, *Rev. Palaeobot. Palynol.*, 198,
471 145–161, doi:10.1016/j.revpalbo.2013.03.004, 2013b.
- 472 Li, J., Servais, T., Yan, K. and Zhu, H.: A nearshore–offshore trend in acritarch distribution from the Early–
473 Middle Ordovician of the Yangtze Platform, South China, *Rev. Palaeobot. Palynol.*, 130(1–4), 141–161,
474 doi:10.1016/j.revpalbo.2003.12.005, 2004.
- 475 Looy, C. V., Twitchett, R. J., Dilcher, D. L., Van Konijnenburg-Van Cittert, J. H. and Visscher, H.: Life in the
476 end-Permian dead zone, *PNAS*, 98(14), 7879–7883, 2001.
- 477 McGhee, G. R., Sheehan, P. M., Bottjer, D. J. and Droser, M. L.: Ecological ranking of Phanerozoic biodiversity
478 crises: The Serpukhovian (early Carboniferous) crisis had a greater ecological impact than the end-Ordovician,
479 *Geology*, 40(2), 147–150, doi:10.1130/G32679.1, 2012.
- 480 Mertens, K. N., Ribeiro, S., Bouimtarhan, I., Caner, H., Combourieu Nebout, N., Dale, B., De Vernal, A.,
481 Ellegaard, M., Filipova, M., Godhe, A., Goubert, E., Grøsfjeld, K., Holzwarth, U., Kotthoff, U., Leroy, S. A. G.,
482 Londeix, L., Marret, F., Matsuoka, K., Mudie, P. J., Naudts, L., Peña-Manjarrez, J. L., Persson, A., Popescu, S.-
483 M., Pospelova, V., Sangiorgi, F., van der Meer, M. T. J., Vink, A., Zonneveld, K. A. F., Vercauteren, D.,
484 Vlassenbroeck, J. and Louwye, S.: Process length variation in cysts of a dinoflagellate, *Lingulodinium*
485 *machaerophorum*, in surface sediments: Investigating its potential as salinity proxy, *Mar. Micropaleontol.*,
486 70(1–2), 54–69, doi:10.1016/j.marmicro.2008.10.004, 2009.
- 487 Mertens, K. N., Dale, B., Ellegaard, M., Jansson, I.-M., Godhe, A., Kremp, A. and Louwye, S.: Process length
488 variation in cysts of the dinoflagellate *Protoceratium reticulatum*, from surface sediments of the Baltic–
489 Kattegat–Skagerrak estuarine system: a regional salinity proxy, *Boreas*, 40(2), 242–255, doi:10.1111/j.1502-
490 3885.2010.00193.x, 2011.
- 491 Mertens, K. N., Bringué, M., Van Nieuwenhove, N., Takano, Y., Pospelova, V., Rochon, A., De Vernal, A.,
492 Radi, T., Dale, B., Patterson, R. T., Weckström, K., Andrén, E., Louwye, S. and Matsuoka, K.: Process length
493 variation of the cyst of the dinoflagellate *Protoceratium reticulatum* in the North Pacific and Baltic-Skagerrak
494 region: calibration as an annual density proxy and first evidence of pseudo-cryptic speciation, *J. Quaternary Sci.*,
495 27(7), 734–744, doi:10.1002/jqs.2564, 2012.
- 496 Mettam, C., Zerkle, A. L., Claire, M. W., Izon, G., Junium, C. J. and Twitchett, R. J.: High-frequency
497 fluctuations in redox conditions during the latest Permian mass extinction, *Palaeogeogr. Palaeoclimatol.*,
498 doi:10.1016/j.palaeo.2017.06.014, 2017.
- 499 Mudie, P. J., Aksu, A. E. and Yasar, D.: Late Quaternary dinoflagellate cysts from the Black, Marmara and
500 Aegean seas: variations in assemblages, morphology and paleosalinity, *Mar. Micropaleontol.*, 43(1–2), 155–178,
501 doi:10.1016/S0377-8398(01)00006-8, 2001.



- 502 Mudie, P. J., Rochon, A., Aksu, A. E. and Gillespie, H.: Dinoflagellate cysts, freshwater algae and fungal spores
503 as salinity indicators in Late Quaternary cores from Marmara and Black seas, *Mar. Geol.*, 190(1), 203–231,
504 doi:10.1016/S0025-3227(02)00348-1, 2002.
- 505 Pacton, M., Gorin, G. E. and Vasconcelos, C.: Amorphous organic matter — Experimental data on formation
506 and the role of microbes, *Rev. Palaeobot. Palyno.*, 166(3–4), 253–267, doi:10.1016/j.revpalbo.2011.05.011,
507 2011.
- 508 Parrish, J. T., Ziegler, A. M. and Scotese, C. R.: Rainfall patterns and the distribution of coals and evaporites in
509 the Mesozoic and Cenozoic, *Palaeogeogr. Palaeocl.*, 40(1), 67–101, doi:10.1016/0031-0182(82)90085-2, 1982.
- 510 Peng, Y., Shi, G. R., Gao, Y., He, W. and Shen, S.: How and why did the Lingulidae (Brachiopoda) not only
511 survive the end-Permian mass extinction but also thrive in its aftermath?, *Palaeogeogr. Palaeocl.*, 252(1–2),
512 118–131, doi:10.1016/j.palaeo.2006.11.039, 2007.
- 513 Piasecki, S.: Preliminary palynostratigraphy of the Permian-Lower Triassic sediments in Jameson Land and
514 Scoresby Land, East Greenland, *B. Geol. Soc. Denmark*, 32, 139–144, 1984.
- 515 Pospelova, V., Chmura, G. L. and Walker, H. A.: Environmental factors influencing the spatial distribution of
516 dinoflagellate cyst assemblages in shallow lagoons of southern New England (USA), *Rev. Palaeobot. Palyno.*,
517 128(1–2), 7–34, doi:10.1016/S0034-6667(03)00110-6, 2004.
- 518 Rodland, D. L. and Bottjer, D. J.: Biotic Recovery from the End-Permian Mass Extinction: Behavior of the
519 Inarticulate Brachiopod *Lingula* as a Disaster Taxon, *PALAIOS*, 16(1), 95–101, doi:10.1669/0883-
520 1351(2001)016<0095:BRFTEP>2.0.CO;2, 2001.
- 521 Sarjeant, W. A. S.: Acritarchs and tasmanitids form the Chhidru Formation, uppermost Permian of West
522 Pakistan, *Stratigraphic Boundary Problems: Permian and Triassic of West Pakistan*, *Spec. Publ.* 4, 277–304,
523 1970.
- 524 Sarjeant, W. A. S. and Stancliffe, R. P. W.: The *Micrhystridium* and *Veryhachium* Complexes (Acritarcha:
525 Acanthomorphae and Polygonomorphae): A Taxonomic Reconsideration, *Micropaleontology*, 40(1), 1–77,
526 doi:10.2307/1485800, 1994.
- 527 Schobben, M., Joachimski, M. M., Korn, D., Leda, L. and Korte, C.: Palaeothys seawater temperature rise and
528 an intensified hydrological cycle following the end-Permian mass extinction, *Gondwana Res.*, 26(2), 675–683,
529 doi:10.1016/j.gr.2013.07.019, 2014.
- 530 Sephton, M. A., Looy, C. V., Brinkhuis, H., Wignall, P. B., De Leeuw, J. W. and Visscher, H.: Catastrophic soil
531 erosion during the end-Permian biotic crisis, *Geology*, 33(12), 941–944, 2005.
- 532 Servais, T., Stricanne, L., Montenari, M. and Pross, J.: Population dynamics of galeate acritarchs at the
533 Cambrian–Ordovician transition in the Algerian Sahara, *Palaeontology*, 47(2), 395–414, doi:10.1111/j.0031-
534 0239.2004.00367.x, 2004.
- 535 Shen, J., Lei, Y., Algeo, T. J., Feng, Q., Servais, T., Yu, J. and Zhou, L.: Volcanic effects on microplankton
536 during the Permian–Triassic transition (Shangsi and Xinmin, South China), *PALAIOS*, 28(8), 552–567,
537 doi:10.2110/palo.2013.p13-014r, 2013.
- 538 Sluijs, A. and Brinkhuis, H.: A dynamic climate and ecosystem state during the Paleocene-Eocene Thermal
539 Maximum: inferences from dinoflagellate cyst assemblages on the New Jersey Shelf, *Biogeosciences*, 6(8),
540 1755–1781, doi:10.5194/bg-6-1755-2009, 2009.
- 541 Stemmerik, L. A. R. S., Bendix-Almgreen, S. E. and Piasecki, S.: The Permian–Triassic boundary in central
542 East Greenland: past and present views." *Bulletin of the Geological Society of Denmark*, *B. Geol. Soc.*
543 *Denmark*, 48(2), 159–167, 2001.
- 544 Stevens, C. H.: Was development of brackish oceans a factor in Permian extinctions?, *Geol. Soc. Am. Bull.*,
545 88(1), 133–138, doi:10.1130/0016-7606(1977)88<133:WDOBOA>2.0.CO;2, 1977.



- 546 Stricanne, L., Munnecke, A., Pross, J. and Servais, T.: Acritarch distribution along an inshore–offshore transect
547 in the Gorstian (lower Ludlow) of Gotland, Sweden, *Rev. Palaeobot. Palyno.*, 130(1–4), 195–216,
548 doi:10.1016/j.revpalbo.2003.12.007, 2004.
- 549 Sun, Y., Joachimski, M. M., Wignall, P. B., Yan, C., Chen, Y., Jiang, H., Wang, L. and Lai, X.: Lethally hot
550 temperatures during the Early Triassic greenhouse, *Science*, 338(6105), 366–370, doi:10.1126/science.1224126,
551 2012.
- 552 Surlyk, F., Piasecki, S., Rolle, F., Stemmerik, L., Thomsen, E. and Wrang, P.: The Permian base of East
553 Greenland, in *Petroleum Geology of the North European Margin*, edited by A. M. Spencer, pp. 303–315,
554 Springer Netherlands., 1984.
- 555 Svensen, H., Planke, S., Polozov, A. G., Schmidbauer, N., Corfu, F., Podladchikov, Y. Y. and Jamtveit, B.:
556 Siberian gas venting and the end-Permian environmental crisis, *Earth Planet. Sc. Lett.*, 277(3–4), 490–500,
557 doi:10.1016/j.epsl.2008.11.015, 2009.
- 558 Tappan, H. and Loeblich, A. R.: Evolution of the oceanic plankton, *Earth-Sci. Rev.*, 9(3), 207–240,
559 doi:10.1016/0012-8252(73)90092-5, 1973.
- 560 Twitchett, R. J.: The Lilliput effect in the aftermath of the end-Permian extinction event, *Palaeogeogr. Palaeocl.*,
561 252(1–2), 132–144, doi:10.1016/j.palaeo.2006.11.038, 2007.
- 562 Twitchett, R. J., Looy, C. V., Morante, R., Visscher, H. and Wignall, P. B.: Rapid and synchronous collapse of
563 marine and terrestrial ecosystems during the end-Permian biotic crisis, *Geology*, 29(4), 351–354,
564 doi:10.1130/0091-7613(2001)029<0351:RASCOM>2.0.CO;2, 2001.
- 565 Tyson, R.: *Sedimentary Organic Matter: Organic facies and palynofacies*, 1995 edition., Springer., 1995.
- 566 Vernal, A. de, Hillaire-Marcel, C., Turon, J.-L. and Matthiessen, J.: Reconstruction of sea-surface temperature,
567 salinity, and sea-ice cover in the northern North Atlantic during the last glacial maximum based on dinocyst
568 assemblages, *Can. J. Earth Sci.*, 37(5), 725–750, doi:10.1139/e99-091, 2000.
- 569 Westerbom, M., Kilpi, M. and Mustonen, O.: Blue mussels, *Mytilus edulis*, at the edge of the range: population
570 structure, growth and biomass along a salinity gradient in the north-eastern Baltic Sea, *Mar. Biol.*, 140(5), 991–
571 999, doi:10.1007/s00227-001-0765-6, 2002.
- 572 Wignall, P. B. and Hallam, A.: Anoxia as a cause of the Permian/Triassic mass extinction: facies evidence from
573 northern Italy and the western United States, *Palaeogeogr. Palaeocl.*, 93(1), 21–46, doi:10.1016/0031-
574 0182(92)90182-5, 1992.
- 575 Wignall, P. B. and Twitchett, R. J.: Oceanic anoxia and the end Permian mass extinction, *Science*, 272(5265),
576 1155, 1996.
- 577 Wignall, P. B. and Twitchett, R. J.: Permian–Triassic sedimentology of Jameson Land, East Greenland: incised
578 submarine channels in an anoxic basin, *J. Geol. Soc.*, 159(6), 691–703, doi:10.1144/0016-764900-120, 2002.
- 579 Winguth, A. and Winguth, C.: Precession-driven monsoon variability at the Permian–Triassic boundary —
580 Implications for anoxia and the mass extinction, *Global. Planet. Change*, 105, 160–170,
581 doi:10.1016/j.gloplacha.2012.06.006, 2012.
- 582 Yin, H., Ed.: *The Palaeozoic-Mesozoic boundary, candidates of Global Stratotype Section and Point of the*
583 *Permian-Triassic boundary*, China University of Geosciences Press, Wuhan., 1996.
- 584 Zonneveld, J.-P., Beatty, T. W. and Pemberton, S. G.: Lingulide Brachiopods and the Trace Fossil *Lingulichnus*
585 from the Triassic of Western Canada: Implications for Faunal Recovery After the End-Permian Mass Extinction,
586 *PALAIOS*, 22(1), 74–97, doi:10.2110/palo.2005.p05-103r, 2007.
- 587 Zonneveld, K. A. F., Marret, F., Versteegh, G. J. M., Bogus, K., Bonnet, S., Bouimetarhan, I., Crouch, E., de
588 Vernal, A., Elshawanay, R., Edwards, L., Esper, O., Forke, S., Grøsfjeld, K., Henry, M., Holzwarth, U., Kieft,



589 J.-F., Kim, S.-Y., Ladouceur, S., Ledu, D., Chen, L., Limoges, A., Londeix, L., Lu, S.-H., Mahmoud, M. S.,
590 Marino, G., Matsouka, K., Matthiessen, J., Mildenhall, D. C., Mudie, P., Neil, H. L., Pospelova, V., Qi, Y., Radi,
591 T., Richerol, T., Rochon, A., Sangiorgi, F., Solignac, S., Turon, J.-L., Verleye, T., Wang, Y., Wang, Z. and
592 Young, M.: Atlas of modern dinoflagellate cyst distribution based on 2405 data points, *Rev. Palaeobot. Palyno.*,
593 191, 1–197, doi:10.1016/j.revpalbo.2012.08.003, 2013.

594

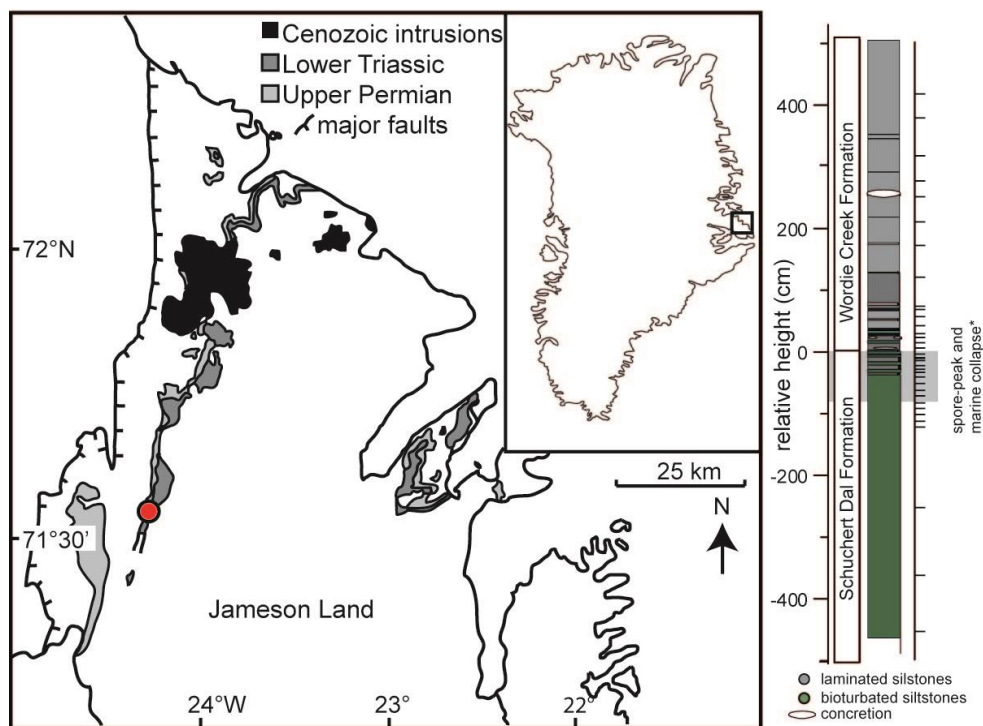
595

596



597 **Figure 1.** Modern map of Jameson Land, East Greenland (adapted from Piasecki, 1984). The location of the
598 studied section is indicated with a red circle. The right panel show the lithology of the Jameson Land section
599 and sample depths. (* spore-peak after Looy et al., 2001, marine collapse after Twitchett et al., 2001).

600



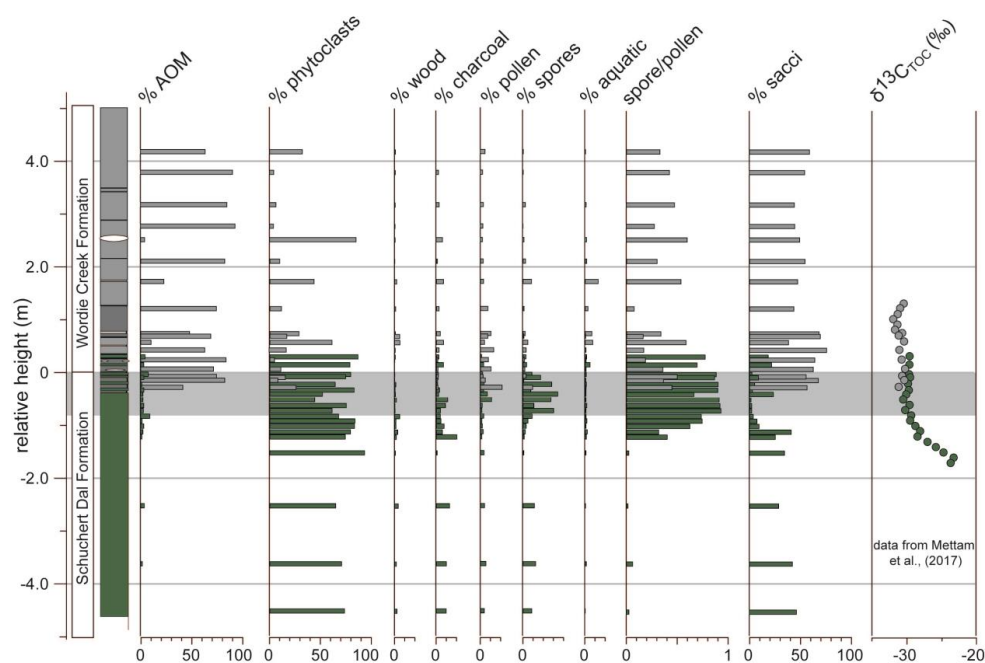
601
602

603

604



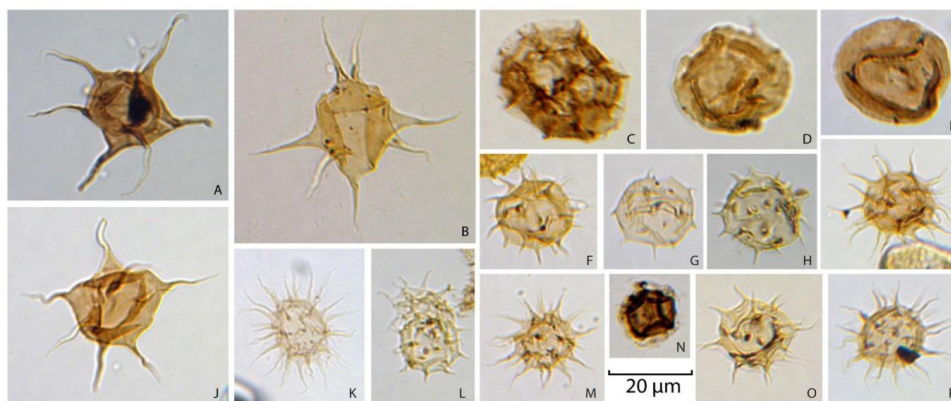
605 **Figure 2.** Change in major groups of palynofacies. AOM= amorphous organic matter. The grey shaded box
606 highlights the biotic crisis as defined by the high spore/pollen ratios, which are indicative for the disappearance
607 of forest communities. Green shading indicates data from bioturbated rocks; grey shading indicates data from
608 laminated rocks. Grey horizontal bar indicates the extinction interval, based on high spore: pollen ratios.
609
610



611
612
613
614
615
616
617



618 **Figure 3.** Aquatic palynomorphs plate. A) *M. pentagonale* – group, B) *V. laidii* - group C) *Cymatiosphaera* sp.
619 D) and E) leiospheres F-I) *M. breve* -group J) *M. pentagonale* - group K)-M) *M. breve* - group N)
620 *Cymatiosphaera* sp. O) and P) *M. breve* -group



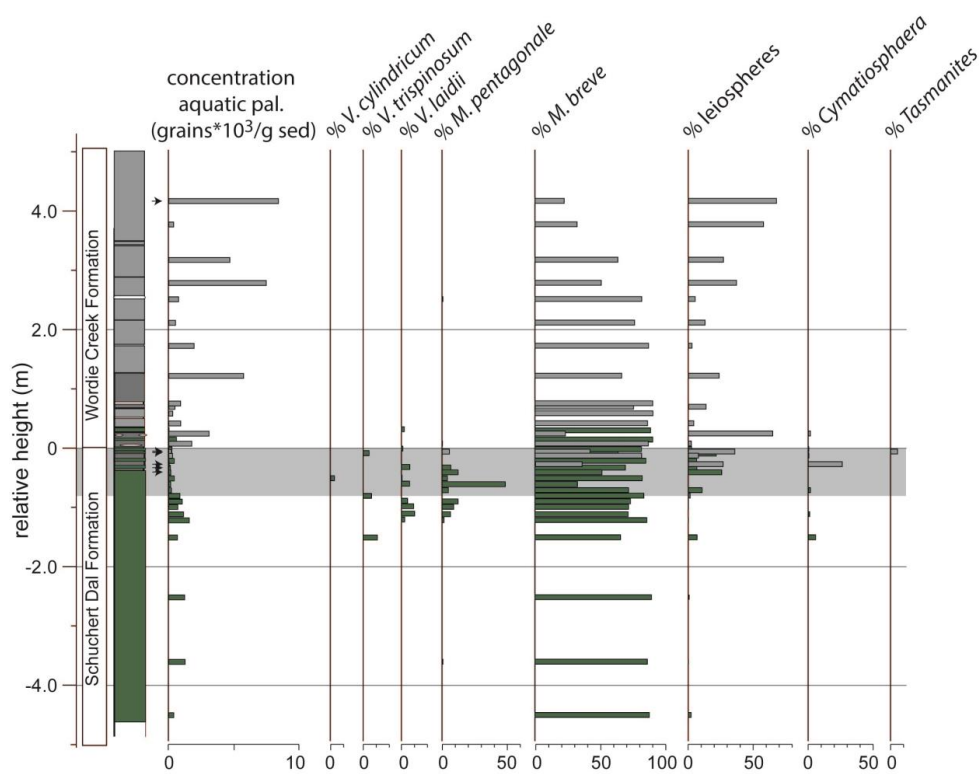
621
622

623

624

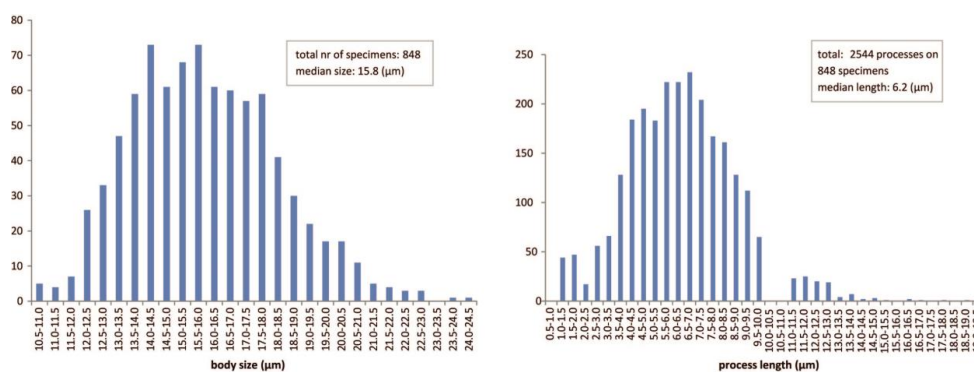


625 **Figure 4.** Aquatic palynomorphs. The figure shows concentration of all aquatic palynomorphs and relative
 626 abundance specific acritarch and prasinophyte groups. Arrow indicate intervals with low counts (<20). Green
 627 shading indicates data from bioturbated rocks; grey shading indicates data from laminated rocks. Grey
 628 horizontal bar indicates the extinction interval, based on high spore: pollen ratios.
 629





632 **Figure 5.** Size-frequency of body diameter (left) and proces length (right).



633

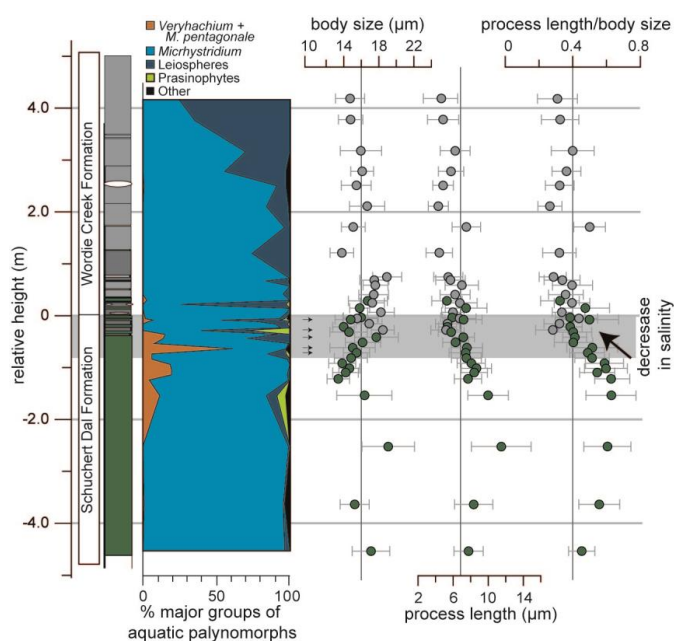
634

635



636 **Figure 6.** Changes in acritarch abundance and morphology. In the panel on the left are the main groups of
 637 aquatic palynomorphs summarized. On the right: body size, process length, and process length relative to
 638 size. Where are low counts? Green shading indicates data from bioturbated rocks; grey shading indicates data
 639 from laminated rocks. The grey bar indicates the extinction interval, based on high spore:pollen ratios. The five
 640 small black arrows indicate in which samples the number of specimens used for measurements was low (4-16
 641 specimens). Grey horizontal bar indicates the extinction interval, based on high spore: pollen ratios.

642
 643



644